CONF-9203208--1

WSRC-MS-92-320

J-INTEGRAL OF CIRCUMFERENTIAL CRACK IN LARGE DIAMETER PIPES (U)

by P. S. Lam, et al.

Westinghouse Savannah River Company
Savannah River Site
Aiken, South Carolina 29808

WSRC-MS--92-320

DE93 003708

G. E. Mertz
Westinghouse Savannah River Company
W. Ji
Department of Mechanical Engineering
Y. J. Chao
Department of Mechanincal Engineering
M. A. Sutton
Department of Mechanical Engineering
University of South Carolina
Columbia, SC

A paper proposed for Presentation/Publication
at the Second International Conference on Nuclear Engineering
San Francisco, CA
03/21-24/92

Available to DOE and DOE contractors from the Office of Scientific and Technical Information, P.O. Box 62, Oak Ridge, TN 37831; prices available from (615) 576-8401, FTS 626-8401.

Available to the public from the National Technical Information Service, U.S. Department of Commerce, 5285 Port Royal Rd., Springfield, VA 22161.

J-INTEGRAL OF CIRCUMFERENTIAL CRACK IN LARGE DIAMETER PIPES

Wei Ji, Yuh J. Chao, Michael A. Sutton
Department of Mechanical Engineering
University of South Carolina
Columbia, South Carolina

P.S. Lam, G.E. Mertz
Westinghouse Savannah River Company
Savannah River Technology Center
Aiken, South Carolina

ABSTRACT

Large diameter thin-walled pipes are encountered in low pressure nuclear power piping system. Fracture parameters, such as K and J, associated with postulated cracks are needed to assess the safety of the structure, for example, prediction of the onset of the crack growth and the stability of the crack. The Electric Power Research Institute (EPRI) has completed a comprehensive study of cracks in pipes and handbook-type data is available. However, for some large diameter, thin-walled pipes the needed information is not included in the handbook. This paper reports our study of circumferential cracks in large diameter, thin-walled pipes (R/t=30 to 40) under remote bending or tension loads. Elastic-Plastic analyses using finite element method were performed to determine the elastic and fully plastic J values for various pipe/crack geometries. A non-linear Ramberg-Osgood material model is used, with strain hardening exponents(n) ranging from 3 to 10. A number of circumferential, through thickness cracks were studied with half crack angles ranging from 0.063π to 0.5π. Results are tabulated for use with the EPRI estimation scheme.

1. INTRODUCTION

1.1 Background

In piping systems, fracture processes generally occur with considerable material yielding. Linear elastic fracture mechanics (LEFM) procedures usually lead to overly conservative predictions and thus result in severe penalties on designs. Hence, elastic-plastic fracture mechanics (EPFM) procedures are necessary to provide more realistic measures of fracture behavior and design margin. However, EPFM analyses require the use of sophisticated finite element methods, which are expensive and time consuming. To overcome these difficulties, an engineering approach was developed by Elestric Power Research Institute (EPRI) [1,2] to provide simple and acceptable solutions to engineers. The EPRI methodology is described in the following sections.

1.2 Elastic-Plastic Engineering Approach

For a Ramberg-Osgood material characterized by:

$$\epsilon/\epsilon_0=\sigma/\sigma_0+\alpha(\sigma/\sigma_0)^n \quad (1)$$

the elastic-plastic estimation formula developed by EPRI combines the linear elastic and fully plastic contributions and is of the form:

$$J(a,P)=J^e(a_e,P)+J^p(a,P) \quad (2)$$

where a is half of the crack length and P is the applied load, $J^e(a_e,P)$ denotes the adjusted elastic contribution, $J^p(a,P)$ represents the fully plastic contribution, a_e is the effective crack length adjusted to include Irwin's small-scale yielding correction and is given by:

$$a_e=a+\phi r_y \quad (3)$$

$$r_y=1/(\beta\pi)[(n-1)/(n+1)](K_I/\sigma_0)^2 \quad (4)$$

$$\phi=1/[1+(P/P_0)^2] \quad (5)$$

and $\beta=2$ for plane sress; 6 for plane strain and P_0 is the limit load corresponding to the perfectly plastic material.

To apply the EPRI methodology, one must obtain estimetes for J^p and J^e. Estimates for J^p are determined by applied load, geometry, material and a dimensionless function h_1 which is obtained by finite element analysis under fully plastic condition and is independent of applied load and material. Estimates for J^e are determined by applied load, geometry, material and a dimensionless function F which is obtained by linear-elastic finite element analysis and is independent of applied load and material also. Because the functions h_1 and F are independent of applied load and material, one can estimate J^p and J^e with certain geometry for any applied load and material once h_1 and F are obtained.

2. APPLICATION OF EPRI APPROACH TO CYLIDERS WITH THROUGH-THICKNESS FLAWS

2.1 Cylinders Under Remote Tension

Consider a cylinder containing a through-wall flaw and subjected to remote uniform tension as shown in Figures 1a and 1b, where R denotes the mean radius, t the wall thickness, 2γ the total crack angle, $2a = 2\gamma R$ is the total length of the crack in the circumferential direction, $2b = 2\pi R$ is the pipe circumference and P is the applied load.

In the linear elastic range, the stress intensity factor K_I due to the crack can be expressed as:

$$K_I = \sigma^*[\pi a]^{1/2}F(a/b,R/t) \quad (6)$$

where $\sigma^* = P/2\pi Rt$, F is a dimensionless function.

J integral can be calculated using plane stress relationship between K_I and J:

$$J^e(a,P) = K_I^2/E \quad (7)$$

Under fully plastic condition, the J-integral is expressed as:

$$J^p(a,P) = \alpha\sigma_0\epsilon_0 c(a/b)h_1(a/b,n,R/t)(P/P_0)^{n+1} \quad (8)$$

where σ_0, ϵ_0 are reference stress and strain respectively, n the strain hardening exponent, h_1 dimensionless function, α a material constant, $2c = 2R(\pi-\gamma)$ is the remaining ligament and P_0 is the limit load for a perfectly plastic material ($n = \infty$) obtained by using the force and moment equilibrium on the cracked section of the cylinder against remotely applied tension. An expression for P_0 is

$$P_0 = 2\sigma_0 Rt[\pi-\gamma-2\arcsin(1/2\sin\gamma)] \quad (9)$$

using equations (2), (6), (7) and (8) one has

$$J(a,P) = f_1(a_e/b,R/t)P^2/E + \alpha\sigma_0\epsilon_0 c(a/b)h_1(a/b,n,R/t)(P/P_0)^{n+1} \quad (10)$$

$$f_1(a/b,R/t) = aF^2(a/b,R/t)/4\pi R^2t^2$$

2.2 Cylinders Under Remote Bending

A cylinder containing a through-wall flaw and subjected to remote bending moment M at its ends (as shown in Figure 2) is handled in a manner similar to the tension loading problem described in section 2.1.

The elastic solution is written:

$$K_I = \sigma^*[\pi a]^{1/2}F(a/b,R/t) \quad (11)$$

where $\sigma^* = MR/I$

$$I = 1/(4\pi)(R_0^4-R_i^4)$$

$$J^e(a,P) = K_I^2/E$$

The fully plastic solution is written:

$$J^p(a,M) = \alpha\sigma_0\epsilon_0 c(a/b)h_1(a/b,n,R/t)(M/M_0)^{n+1} \quad (12)$$

where M_0 is the limit moment for a cracked pipe under pure bending corresponding to perfect plastic material $n = \infty$, and is written:

$$M_0 = M_0'[\cos(\gamma/2)-1/2\sin(\gamma)] \quad (13)$$

and $M_0' = 4\sigma_0 R^2t$ is the limit moment of an uncracked cylinder. Using equations (2), (11) and (12) one can write

$$J(a,M) = f_1(a_e/b,R/t)M^2/E + \alpha\sigma_0\epsilon_0 c(a/b)h_1(a/b,n,R/t)(M/M_0)^{n+1} \quad (14)$$

$$f_1(a/b,R/t) = \pi a(R/I)^2F^2(a/b,R/t)$$

3. EVALUATION OF CIRCUMFERENTIAL, THROUGH-THICKNESS FLAWS IN THIN-WALLED CYLINDERS

3.1 Calculation For Functions F And h_1

In EPRI report [2], finite element analyses were conducted to calculate the dimensionless functions F(a/b,R/t) and h_1(a/b,n,R/t). The available data covers the R/t ratio from 5 to 20, a/b from .063 to .5, and material hardening exponents n from 1 to 7.

This work extends the range of coverage for functions F and h_1 (EPRI reports [1,2]) to handle large diameter, thin-walled pipes which are encountered in low pressure nuclear power piping system. The F and h_1 functions were calculated at (a) R/t = 30 and 40; (b) a/b = 0.0625, 0.10, 0.125, 0.175, 0.20, 0.25, 0.30, 0.35, 0.40, 0.45 and 0.50 and (c) material strain hardening exponents n = 3, 5, 7 and 10.

The ABAQUS finite element program [3] was used to carry out detailed analyses, to estimate F and h_1 for the ranges of R/t, a/b and n discussed above. The through-wall cracked cylinders were modeled by 9 node thin shell elements S9R5. Because of symmetry, only a quarter of the cylinder was modeled. Figure 3 represents a typical finite element mesh employed in the analysis. For the case of a/b = 0.175, it consists of 384 S9R5 elements with a total of 1599 nodes. Other meshes were similar and consisted of approximately the same number of elements. F and h_1 functions were obtained by using the elastic and the fully plastic J-integrals, respectively, which were calculated by the finite element analyses.

For cylinders under remote tension, the value of F was estimated using

$$F = K_I/[\sigma^\infty(\pi a)^{1/2}] = [JE]^{1/2}/[\sigma^\infty(\pi a)^{1/2}] \quad (15)$$

and h_1 was obtained from the formula

$$h_1 = J/[\alpha\sigma_0\epsilon_0 c(a/b)(P/P_0)^{n+1}] \quad (16)$$

For cylinders under remote bending, F is again given by equation (15), but h_1 is written

$$h_1 = J/[\alpha\sigma_0\epsilon_0 c(a/b)(M/M_0)^{n+1}] \quad (17)$$

Results for F and h_1 functions obtained are tabulated in Tables 1, 2, 3, 4, 5 and 6.

3.2 Verification Of Results For F And h_1

Elastic-Plastic J-integrals for several prototypic pipe sizes 16"OD, .5"thick (R/t=15.5); 20"OD, .375"thick (R/t=26.167); 24"OD, .375"thick (R/t=31.5) and 42"OD, .5"thick (R/t=41.5) with half crack angle $\gamma = .183\pi$ (a/b=0.183), $\gamma = .25\pi$ (a/b=.25) and $\gamma = .47\pi$ (a/b=0.47) were calculated using both finite element analyses and the EPRI estimation procedure using results in Tables 1 to 6 under bending loads from 0 to twice limit loads ($M/M_0 = 2$). The hardening exponent n=5, $E = 30 \times 10^6$ lb/in², $\nu = 0.3$, $\sigma_0 = 40 \times 10^3$ lb/in², $\alpha = 0.5$. As noted in previous section, the EPRI estimation procedure for J-integral under bending load is equation (14).

The F and h_1 functions for these specific cases were obtained by bilinear interpolation of the F and h_1 data in Tables 2, 5, 6 and EPRI report [2]. In equation (4), β was chosen to be 4 to represent a condition between plane stress ($\beta = 2$) and plane strain ($\beta = 6$). The J-integrals estimated by the bilinear interpolation and equation (14) were compared with those calculated by direct finite element method. The comparison is illustrated in Figures 4, 5 and 6.

As seen in Figures 4, 5 and 6, the results based on EPRI estimationprocedure agree reasonably well with the results from finite element method. Therefore, the EPRI estimation procedure of elastic-plastic J-integral analysis has been extended to larger diameter thin-walled pipes up to R/t=40.

4. CONCLUSIONS

The EPRI estimation scheme for estimation of the applied J-integral values for pipes with circumferential, through-thickness flaws under either tension or bending loads has been extended to include the range $20 \le R/t \le 40$, $3 \le n \le 10$ and $.0625 \le a/b \le .50$.

5. ACKNOWLEDGEMENT

The information contained in this paper was developed during the course of work under Contract No.DE-AC09-89SR18035 with the U.S. Department of Energy and through the South Carolina Universities Research and Education Foundation (SCUREF).

6. REFFERENCES

[1] V. Kumar, M.D. German and C.F. Shih, An Engineering Approach for Elastic-Plastic Fracture Analysis, EPRI NP-1931, 1981

[2] V. Kumar, M.D. German, W.W. Wilkening, W.R. Andrews, H.G. deLorenzi and D.F. Mowbray, Advances in Elastic-Plastic Fracture Analysis, EPRI NP-3607, 1984

[3] ABAQUS Finite Element Program, Version 4-9-1, Hibbitt, Karlsson & Sorensen, Inc.

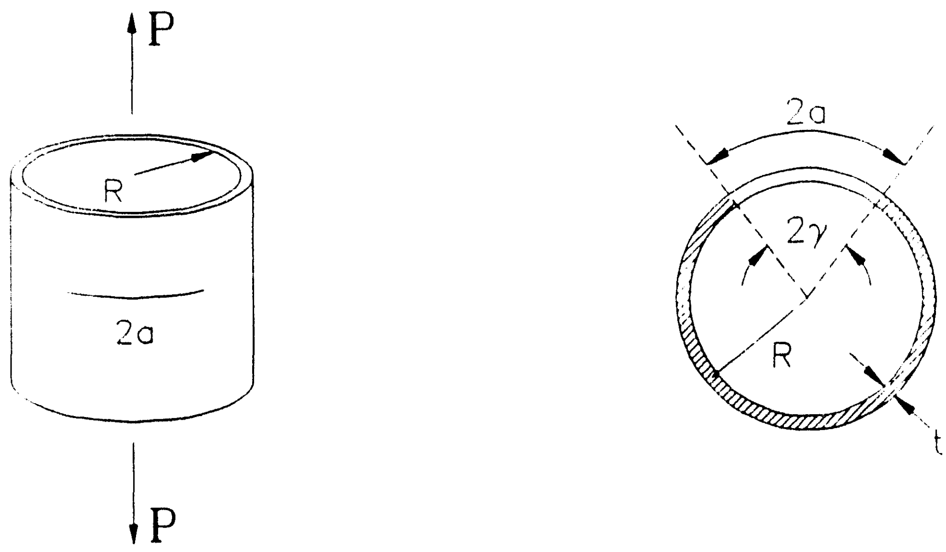

(a) (b)

FIGURE 1. (a) THROUGH-WELL FLAWED CYLINDER UNDER REMOTE TENSION; (b) SCHEMATIC OF CROSS SECTION OF CYLINDER

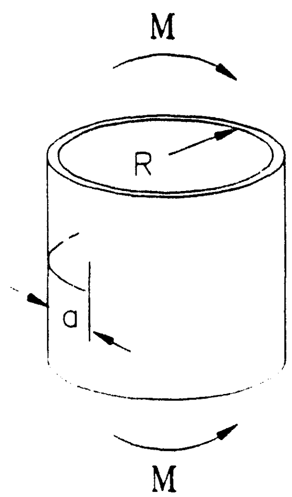

FIGURE 2.THROUGH-WELL FLAWED CYLINDER UNDER REMOTE BENDING

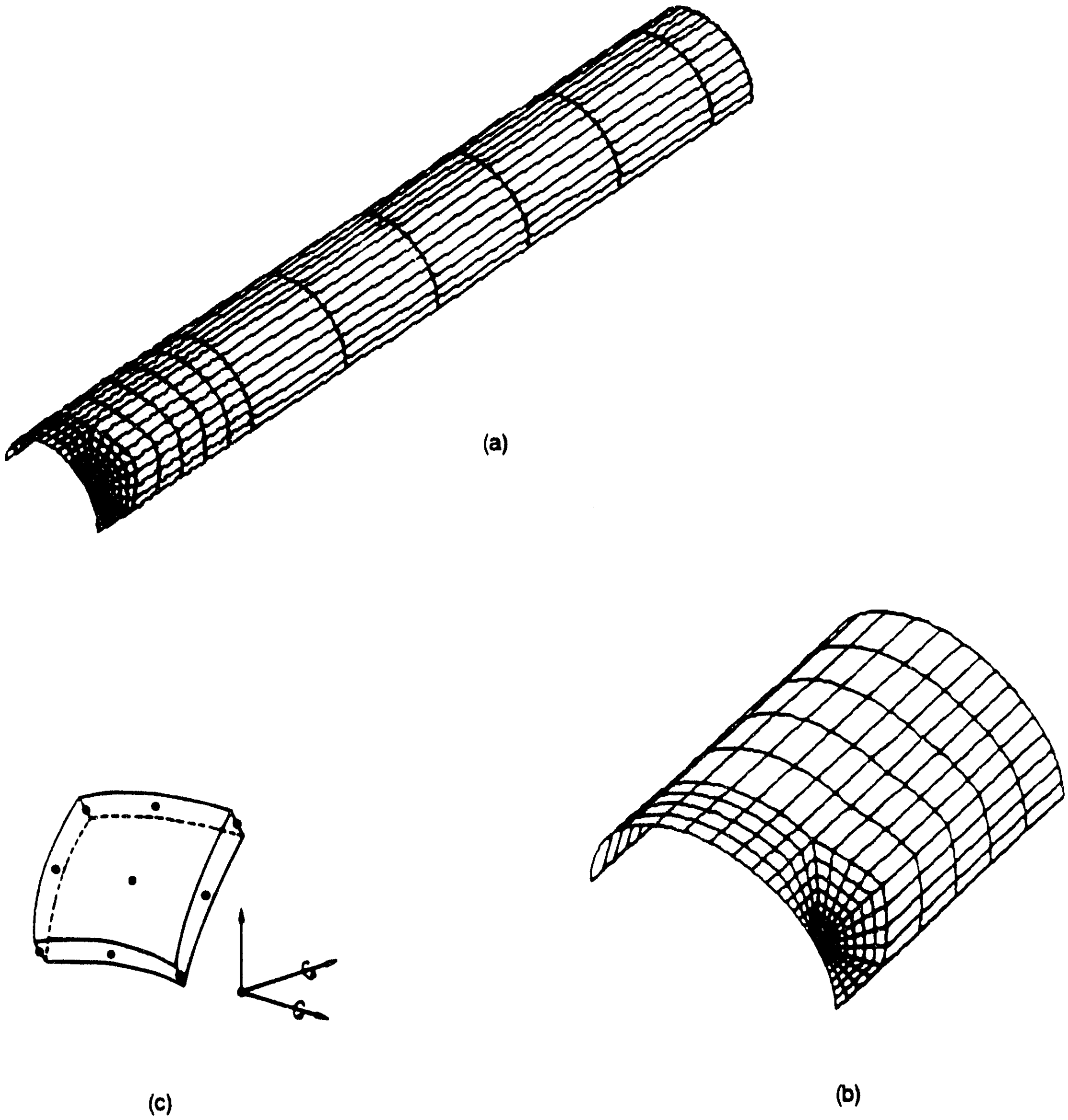

FIGURE 3. (a) FINITE ELEMENT MODEL OF A CYLINDER CONTAINING A CIRCUMFERENTIAL CRACK; (b) DETAILED FINITE ELEMENT MESH AROUND CRACK TIP; (c) 9 NODE SHELL ELEMENT S9R5

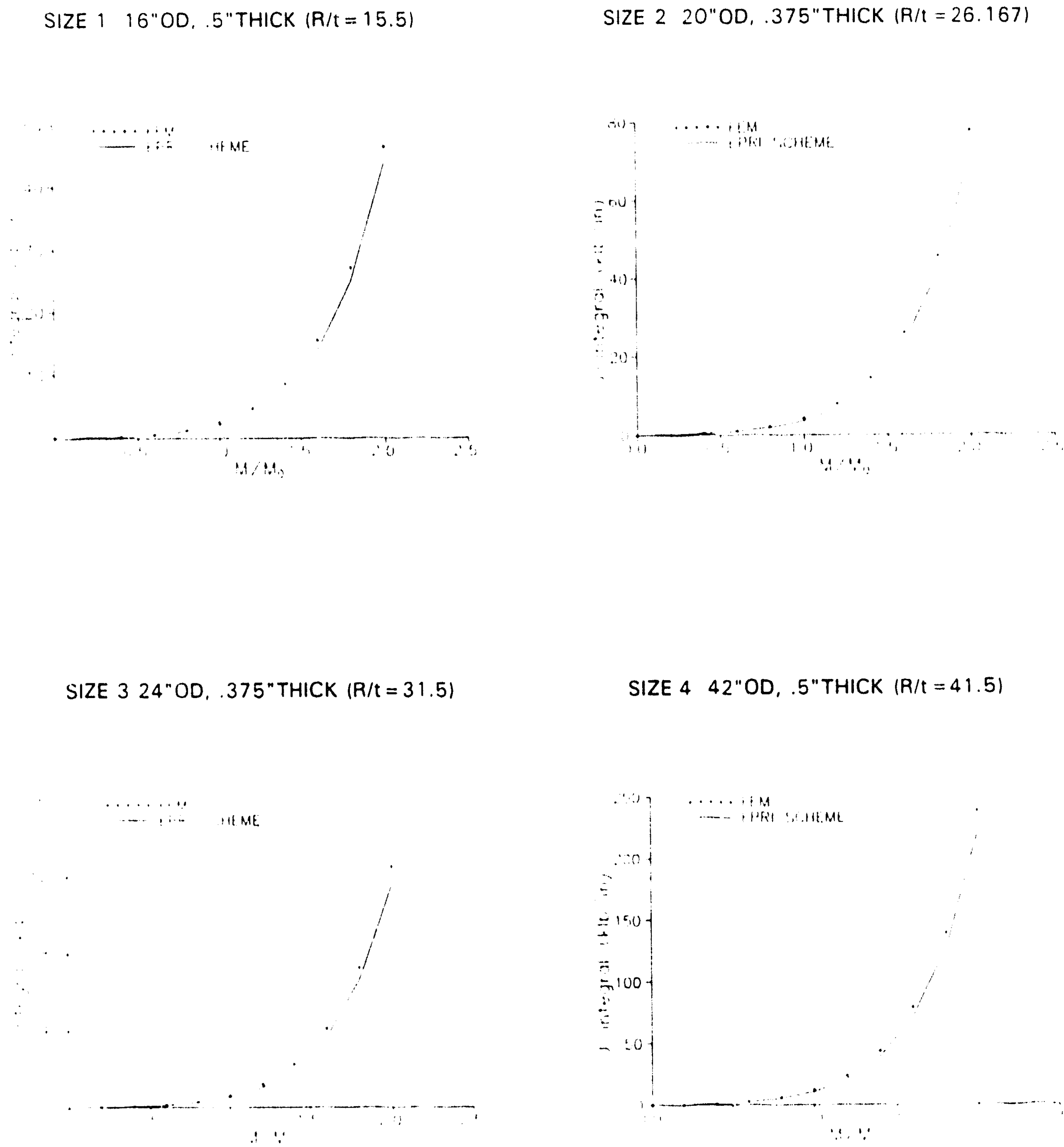

FIGURE 4. COMPARISON OF ENGINEERING APPROACH TO FINITE ELEMENT METHOD AT a/b = .183

SIZE 1 16"OD, .5"THICK (R/t = 15.5)

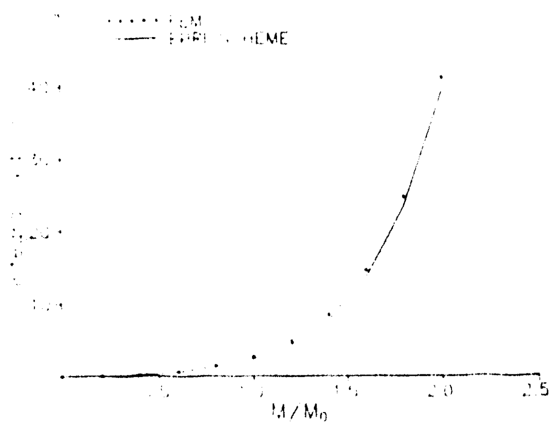

SIZE 2 20"OD, .375"THICK (R/t = 26.167)

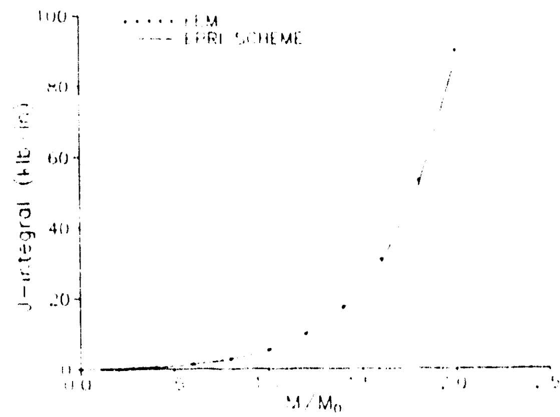

SIZE 3 24"OD, .375"THICK (R/t = 31.5)

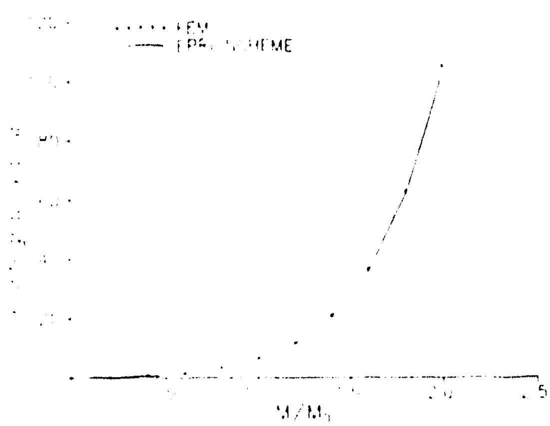

SIZE 4 42"OD, .5"THICK (R/t = 41.5)

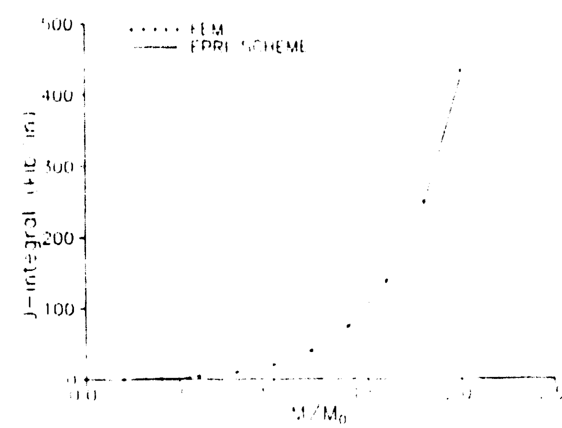

FIGURE 5. COMPARISON OF ENGINEERING APPROACH TO FINITE ELEMENT METHOD AT a/b = .25

SIZE 1 16"OD, .5"THICK (R/t = 15.5)

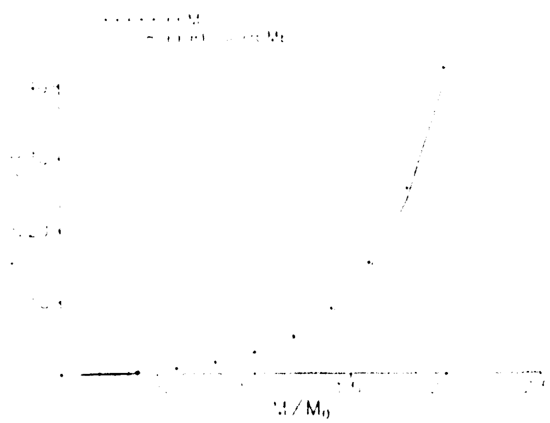

SIZE 2 20"OD, .375"THICK (R/t = 26.167)

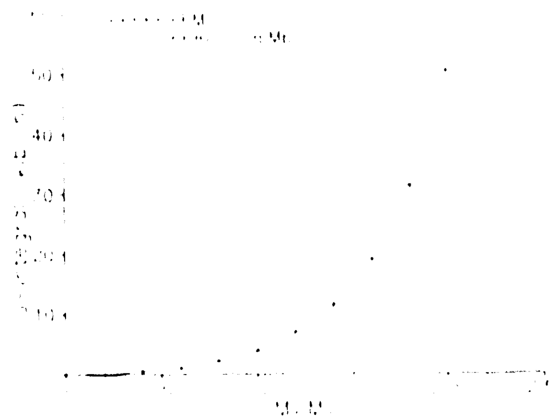

SIZE 3 24"OD, .375"THICK (R/t = 31.5)

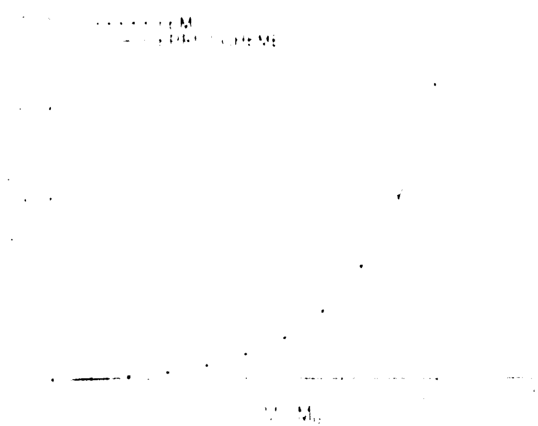

SIZE 4 42"OD, .5"THICK (R/t = 41.5)

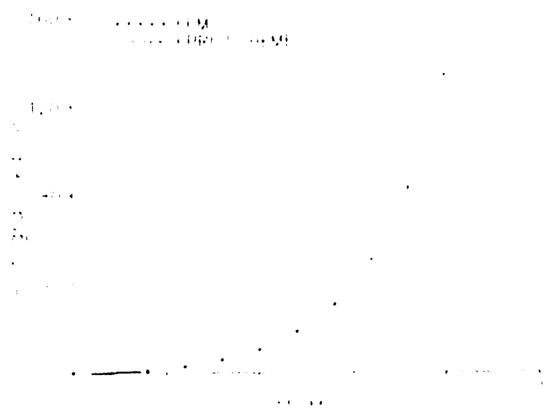

FIGURE 6. COMPARISON OF ENGINEERING APPROACH TO FINITE ELEMENT METHOD AT a/b = .47

TABLE 1. F-FUNCTIONS FOR TENSION

a/b	R/t = 30	R/t = 40
0.0625	1.096	1.072
0.10	1.275	1.269
0.125	1.408	1.411
0.15	1.542	1.558
0.175	1.685	1.711
0.20	1.835	1.871
0.25	2.165	2.233
0.30	2.558	2.697
0.35	3.020	3.189
0.40	3.592	3.760
0.45	4.319	4.544
0.50	5.269	5.567

TABLE 2. F-FUNCTIONS FOR BENDING

a/b	R/t = 30	R/t = 40
0.0625	1.165	1.206
0.10	1.336	1.406
0.125	1.453	1.540
0.15	1.572	1.671
0.175	1.680	1.791
0.20	1.794	1.913
0.25	2.021	2.157
0.30	2.272	2.422
0.35	2.539	2.705
0.40	2.850	3.043
0.45	3.230	3.447
0.50	3.713	3.963

TABLE 3. h_1-FUNCTIONS FOR TENSION (R/t = 30)

a/b	n = 3	n = 5	n = 7	n = 10
.0625	6.25	7.94	9.01	9.74
.10	7.24	8.83	9.23	9.16
.125	7.64	8.77	8.66	7.76
.15	7.76	8.03	7.81	6.37
.175	7.66	7.42	6.57	5.40
.20	7.41	6.64	5.63	4.54
.25	6.67	5.35	4.36	3.45
.30	5.65	4.18	3.36	2.53
.35	4.54	3.34	2.60	1.92
.40	3.78	2.72	2.12	1.58
.45	3.16	2.21	1.71	1.24
.50	2.66	1.84	1.40	1.01

TABLE 4. h_1-FUNCTIONS FOR TENSION (R/t = 40)

a/b	n = 3	n = 5	n = 7	n = 10
.0625	6.87	8.62	9.98	11.70
.10	8.17	9.85	10.71	10.55
.125	8.60	9.73	9.74	8.84
.15	8.73	9.34	8.63	7.43
.175	8.63	8.32	7.41	6.03
.20	8.22	7.48	6.29	5.12
.25	7.51	6.05	4.94	3.91
.30	6.42	4.79	3.85	2.95
.35	5.22	3.81	3.00	2.27
.40	4.30	3.13	2.45	1.83
.45	3.59	2.54	1.95	1.45
.50	3.02	2.10	1.61	1.20

TABLE 5. h_1-FUNCTIONS FOR BENDING (R/t = 30)

a/b	n = 3	n = 5	n = 7	n = 10
.0625	8.81	10.62	11.61	12.56
.10	10.14	11.48	11.79	10.73
.125	10.30	11.11	10.60	9.33
.15	10.21	9.90	9.19	7.52
.175	9.56	8.99	7.87	6.48
.20	8.93	7.89	6.80	5.57
.25	7.92	6.64	5.58	4.40
.30	6.91	5.50	4.41	3.47
.35	5.86	4.45	3.51	2.66
.40	4.91	3.65	2.86	2.14
.45	4.10	2.98	2.31	1.65
.50	3.40	2.33	1.85	1.33

TABLE 6. h_1-FUNCTIONS FOR BENDING (R/t = 40)

a/b	n = 3	n = 5	n = 7	n = 10
.0625	9.93	12.25	13.88	15.06
.10	11.70	13.17	13.69	12.64
.125	11.92	12.79	12.35	10.70
.15	11.69	11.20	11.02	8.74
.175	10.87	10.13	8.81	7.49
.20	9.99	8.80	7.54	6.24
.25	8.94	7.53	6.28	4.93
.30	7.88	6.28	5.09	3.90
.35	6.68	5.11	4.05	3.09
.40	5.61	4.20	3.26	2.49
.45	4.69	3.42	2.69	1.94
.50	3.88	2.77	2.21	1.60

END

DATE FILMED

3 / 16 / 93